A Clustering Genetic Algorithm for Actuator Optimization in Flow Control

Michele Milano
Institute of Computational Sciences, ETH Zentrum
Zürich, CH-8092, Switzerland
milano@eniac.ethz.ch

Petros Koumoutsakos
Institute of Computational Sciences, ETH Zentrum
Zürich, CH-8092, Switzerland
and Center for Turbulence Research
NASA Ames 202A-1
Moffett Field, CA 94035, USA
petros@eniac.ethz.ch

Abstract

Active flow control can provide a leap in the performnace of engineering configurations. Although a number of sensor and actuator configurations have been proposed the task of identifying optimal parameters for control devices is based on engineering intuition usually gathered from uncontrolled flow experiments. Here we propose a clustering genetic algorithm that adaptively identifies critical points in the controlled flow field and adjusts the actuator parameters through an evolutionary process.

We demonstrate the capabilities of the algorithm for the fundamental prototypical problem of an actively controlled circular cylinder. The flow is controlled using surface-mounted vortex generators; the actuators used are belts mounted on the cylinder surface, that modify the tangential velocity on the cylinder surface, and jet actuators, that modify the normal velocity component on the surface. The proposed Genetic Algorithm performs the optimization of the actuators parameters, yielding up to 50% drag reduction. At the same time the Genetic Algorithm performs a sensitivity analysis of the optima it finds, thus allowing a deeper understanding of the underlying physics and also an estimation of which actuator would be easier to implement in a real experiment.

1. Introduction

The flow past a circular cylinder is a well established prototypical configuration of bluff body flows [16]. Here, for the first time, we use evolutionary algorithms in conjunction with CFD to achieve drag reduction in active flow control through modification of the tangential velocity on the cylinder surface.

Several control methodologies have been suggested to modify vortex shedding behind a circular cylinder and to effectuate drag reduction, either with passive geometrical modifications and/or with an open loop steady forcing. A non-exhaustive list includes studies of the effect of a splitter plate attached to the cylinder studied, among others, by [9, 20, 1, 2]. These studies achieved drag reductions from 20 to 40% depending on the arrangement of the control devices. A free rotating cylinder attached to a splitter plate was considered in [6]. The placement of a small secondary cylinder in the wake was shown to suppress the vortex shedding while reducing the drag coefficient [18]. Another possible action is base suction/blowing [17]. Rotational oscillations were studied by [19, 4]. At Reynolds numbers $Re = 15000$ (Re indicates the degree of flow turbulence) and for certain parameters, found after extensive experimentation, this control action was found to induce dramatic changes in the wake and a significant drag reduction of about 60 %. Due to experimental limitations, however, it was not possible to reveal the underlying governing mechanisms .

While a wealth of different possible geometry modifications and/or open loop actions have been devised and studied, little effort has been devoted to algorithms optimizing the various control parameters. Recent CFD studies of suboptimal control [10] have tried to remedy this situation for simulation of flows using mass transpiration as an actuation mechanism. Drag reduction of up to 20% was achieved using this optimization strategy for idealized blowing/suction actuators.

In practice, however, it remains an almost impossible task even to cast the optimization problem in a tractable explicit analytical form for all different types of sensor and actuator devices. The dependence of the control on the type of actuators also minimizes the generalization of certain successful control strategies. Hence, most present day design strategies rely mainly on trial and error experiments, driven by human intuition derived from physical understanding of the phenomenon. This approach has the fundamental limitation that most of this understanding is based on simulations and experiments of the *uncontrolled* flow. Moreover when the placement of the actuators needs to be optimized the cost function can be evaluated only for a certain actuator arrangement and hence no analytical objective function can be prescribed *a priori* in order to be optimized with gradient based techniques. This motivates our interest in automatic optimizers of the *controlled* flow that compactly encode information about desired flow behavior in their objective function.

We conduct two-dimensional simulations for Reynolds number $Re = 500$. Two types of actuators are considered: ideal jet actuators, performing a blowing/suction action on the cylinder surface, and tangential belt actuators, that modify the surface tangential velocity. A study of the effect of the tangential belt actuators has been performed in [5]; in that study the actuators are just sliding walls, driven by the fluid itself and not by an external force. The effect of a belt actuator on drag reduction has been experimentally studied in [3]; in that study a drag reduction has been observed in an oil channel, for a flat wall.

The paper is organized as follows: Section 2 presents flow equations, related numerical parameters of the flow solver and the calculation of the drag coefficient which constitutes the objective function to be minimized. In Section 3 we describe the Genetic Algorithm and the problem setup: we consider an array of actuators placed on the cylinder surface; the Genetic Algorithm incorporates a mutation probability dependent on the distance from a prescribed target value of the objective function. Section 4 describes the results we obtain for tangential belt actuators and jet actuators. Some conclusions are presented in Section 5.

2. Governing equations and numerical method

We consider two-dimensional incompressible viscous flow past a circular cylinder. Governing equations are the Navier-Stokes equations in the velocity-pressure formulation

$$\frac{d\mathbf{v}}{dt} + (\mathbf{v}\cdot\nabla)\mathbf{v} = -\frac{1}{\rho}\nabla P \; + \; \nu\,\nabla^2\mathbf{v} \tag{1}$$

$$\nabla\cdot\mathbf{v} = 0 \tag{2}$$

where $\mathbf{v}$ is the velocity vector, P, ρ is the pressure and density of the flow and ν denotes the kinematic viscosity.

The boundary conditions are defined as:

$$\mathbf{v}(\mathbf{x},t) = \mathbf{V}_{ext} \qquad \text{on the cylinder surface} \tag{3}$$

$$\mathbf{v}(\mathbf{x},t) \; = \; U_\infty\,\mathbf{e}_x \qquad \text{as } |\mathbf{x}| \to \infty \tag{4}$$

where $\mathbf{V}_{ext}$ is the surface velocity induced by the actuators, and $\mathbf{e}_x$ is the unit vector in the stream-wise direction. U_∞ denotes the free-stream velocity. The Reynolds number and Strouhal frequency of the flow are defined as :

$$Re = \frac{U_\infty\,D}{\nu} \qquad\qquad St \; = \; \frac{f\,D}{U_\infty}$$

where $D \; = \; 2\,R$ is the diameter of the cylinder and f the shedding frequency of the flow.

We also define a normalized time, by scaling time as follows:

$$t^* = \frac{t}{t_a} = \frac{t}{(D/U_\infty)}$$

where t_a is the time taken by a fluid particle in the free stream to be advected past the cylinder. The definition of such normalized quantities allows a ready generalization of the results to differently scaled geometries.

The flow solver used in this work [12] employs a staggered, second order central-difference method in generalized coordinates. The solution is advanced in time using a fractional step scheme, in which a third order Runge-Kutta scheme is used for the nonlinear convection terms and a Crank-Nicholson scheme is used for the viscous terms. A multigrid solver is used in conjunction with a Gauss-Seidel line-zebra scheme to solve the pressure Poisson equation.

We focus on the problem of reducing the drag, represented by the drag coefficient C_D calculated from quantities measured on the cylinder surface as:

$$C_D \; = \; \frac{2}{\rho U_\infty^2 D}\int_{cyl}(p\mathbf{n}_{\mathrm{x}} - \tau_{ix}\mathbf{n}_{\mathrm{i}})dl \tag{5}$$

where p is the pressure and τ_{ix} the viscous stress tensor on the surface of the cylinder and $\mathbf{n}_{\mathrm{i}}, i = x, y$ denotes the components of the unit normal on the surface of the cylinder.

3. Problem setup

3.1. The flow solver and the objective function

We consider flow at $Re \; = \; 500$, past a cylinder whose surface is subdivided in $n \;\; = \;\; 16$ equal size segments

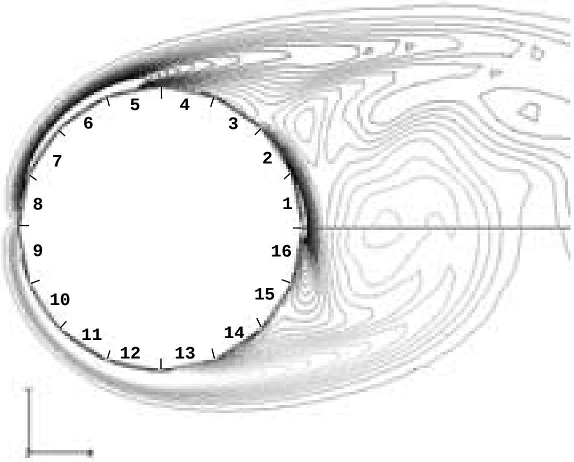

Figure 1. Location of the actuators on the cylinder surface. The belts are numbered as specified in the figure; also a snapshot of the uncontrolled vorticity is reported: the flow is from left to right.

that are allowed either to move tangentially to the cylinder surface, each with a different but steady velocity, or to blow/suck steadily. In the latter case, a zero net mass flow is imposed on the cylinder surface.

The tangential actuation configuration can be physically realized by using a set of moving belts covering the surface of the cylinder. It has been found experimentally by [3] and [13] that such actuators are very efficient in achieving significant drag reduction. Fig.1 shows the location of the belts on the cylinder surface for the case study considered here.

An off-line optimization is performed here for the functional in Eq. 5; the objective function that we optimize is the time average of the drag in a fixed time interval. The average drag is computed at each simulation step, starting from a steady uncontrolled situation and averaging over 4 Strouhal periods.

3.2. The Genetic Algorithm

We use a genetic algorithm (GA) [8, 7] that was specifically designed to find a basin in parameter space containing all parameter configurations yielding fitness values below a given threshold [11].

We study whether this GA can automatically identify critical points such as the separation points of the uncontrolled flow. For $Re = 500$ these points are encompassed by segments 4 and 13.

3.3. GA Description

The GA used in this paper is a modification of Controlled Random Search (CRS) [14]. The algorithm is outlined in the following paragraphs.

Let $G(\lambda)$ the function to be minimized, $\lambda \in R^n$ the parameter vector. In a first phase S population points are initially randomly chosen according to a uniform distribution within a defined search volume of dimension n. The inequality $S \gg n$ must hold for the algorithm to work properly. Then the algorithm proceeds as follows:

1) Choose the population point λ_{max} in which G reaches the maximum value:
$\lambda_{max} = arg\,[\max_{i=1,\ldots,M} G(\lambda_i)]$;
$G_{max} = G(\lambda_{max})$;

2) Randomly choose $n+1$ different population points: $\lambda_1, \ldots, \lambda_{n+1}$ (breeding set). All subsequent operations are performed on this set;

3) Mutation step: for all breeding set points, with probability
$P_i = (1-\alpha^I) \cdot \left(1-\beta^{\frac{(G(\lambda_i)-G_T)}{\overline{G}}}\right) \cdot \gamma$, replace the point λ_i with one randomly chosen within the search volume limits;

4) Recombination step: for each of the $n+1$ points determine the centroid, $\underline{\lambda_i}$, of the other n points, i.e. $\underline{\lambda_i} = \frac{1}{n}\sum_{j=1}^{n} \lambda_j$;

4.a) Generate offspring $\lambda_{si} = 2\underline{\lambda_i} - \lambda_{n+1}$; if λ_{si} is not contained in the search volume, process next point in breeding set ;

4.b) Calculate $G(\lambda_{si})$: if $G(\lambda_{si}) < G_{max}$ then purge λ_{max} from population, and substitute by offspring λ_{si};

5) Compute the new G_{max}, if necessary;

6) Iterate steps 4 and 5 on the whole breeding set;

7) If convergence test fails, return to step 1.

There are 4 parameters, i.e. α, β, γ, G_T and 2 variables: I and $\overline{G}$ to be defined in this scheme. The variable I is the number of consecutive iterations in which the population has not changed, i.e., no offspring has substituted any population member. It provides an empirical measure of the need for fresh information through increased mutation probability. The variable $\overline{G}$ is the average population fitness, used as a scaling factor.

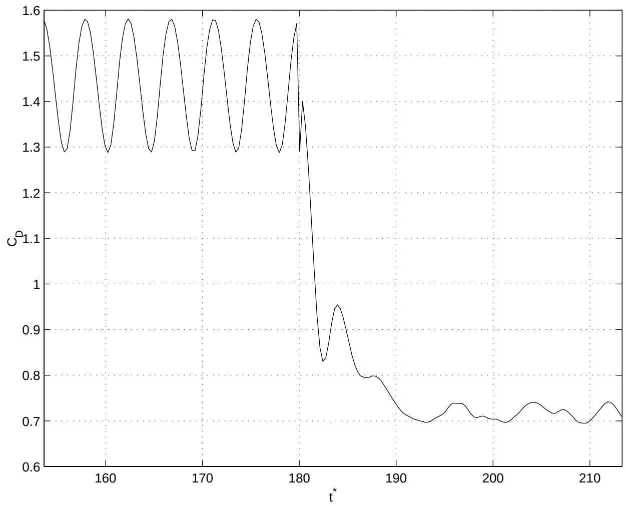

Figure 2. Validation run for the best population member. Control is switched on at $t^* = 180$.

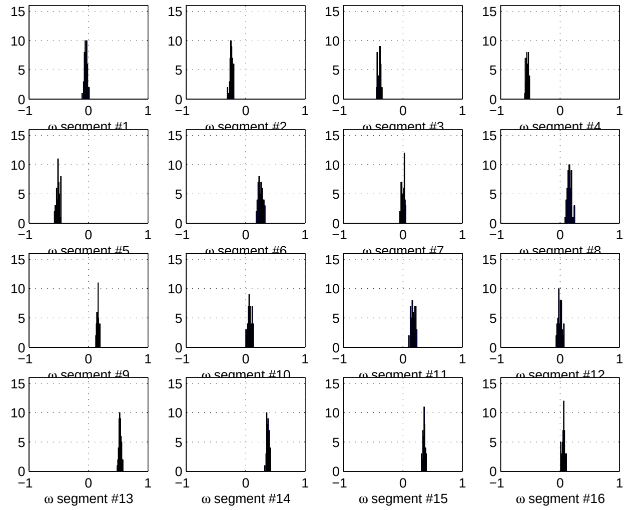

Figure 3. Histogram of the final population cluster: number of population members (ordinates) attaining a given tangential velocity, reported in the abscissas. Segments 4 and 13 contain the flow separation point.

The most important parameter is G_T, a threshold C_D value used for the convergence test: we declare convergence once all of the population's fitness values are below it. Given this criterion, population points will be clustered inside the domain defined as: $\{\lambda | G(\lambda) < G_T\}$. The final cluster provides a sampling of the minimum basin. This allows to retrieve parameter correlations and other meaningful quantities.

According to the formula defining mutation probability, the parameter $0 <= \alpha <= 1$ modulates the mutation rate during the course of the optimization process, and the parameter $0 <= \gamma <= 1$ enforces its upper bound, since $0 <= \beta <= 1$. The term containing the parameter β causes population members far from convergence (with fitness $> G_T$) to mutate more frequently. (CRS can be regarded as a GA with zero mutation probability.)

4. Results

4.1. Tangential belts actuation

For a GA population of 50 elements the parameters α and β were fixed to 0.25, the upper bound γ to 0.02 and the threshold G_T to 0.7. This value is about 50% of the drag coefficient reported for and uncontrolled flow around a cylinder at $Re = 500$ (Panton, 1996). The optimization lasted for 1500 iterations, corresponding to about 30 hours of CPU-time on a NEC SX-4 supercomputer.

On a grid twice as fine as the one used for optimization, a validation run was performed for the best candidate in the population. Fig. 2 plots the behavior of the drag coefficient during the transition from the uncontrolled and controlled phase. The transition phase is quite short, and the flow appears to settle quickly to the minimal drag configuration. The shedding frequency is drastically modified while the fluctuating amplitude in the drag coefficient is significantly reduced.

Fig. 3 shows a histogram of the converged population. We observe that the GA discovered that segments on opposite sides of the cylinder must rotate in opposite directions, in order to delay separation by allowing the flow to "slide" further on the cylinder surface.

This separation delay also becomes obvious by comparing the time averages of the controlled and uncontrolled vorticity contours, shown in Figs 4 and 5, respectively. The controlled wake is more elongated, a clear evidence of a later separation, resulting in a smaller drag.

4.2. Results with jet actuators

In the case of blowing/suction actuation, all the GA parameters including the threshold G_T were kept equal to the case of the tangential actuation, in order to consistently compare the optimization performance.

In this case the GA did not converge to the desired threshold and the mutation probability is saturated to its maximum allowed value, as it is clear from fig. 6. This is an evidence that there is an high probability that the minimum reached is a global one.

An histogram of the final population cluster is shown in fig. 7. In this case the most evident clustering can be ob-

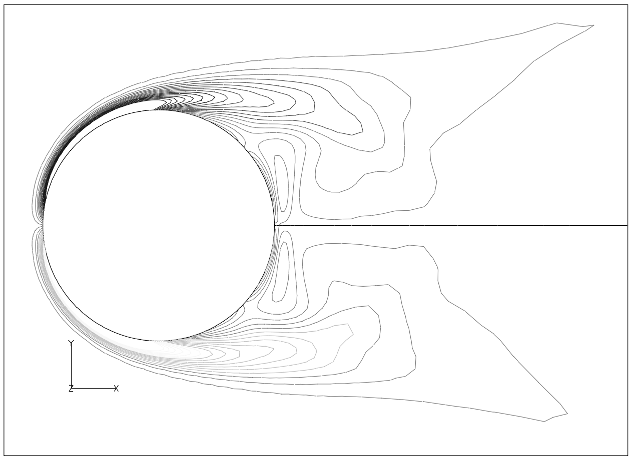

Figure 4. Vorticity contours at $Re = 500$ averaged over 4 Strouhal periods, uncontrolled case.

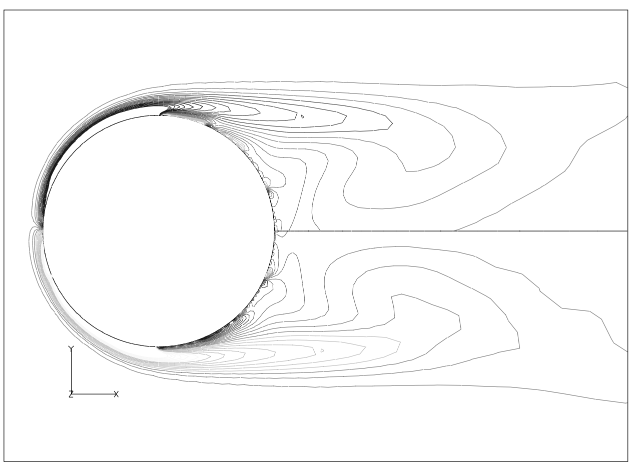

Figure 5. Steady state vorticity contours averaged over 4 Strouhal periods, controlled case using belt actuators.

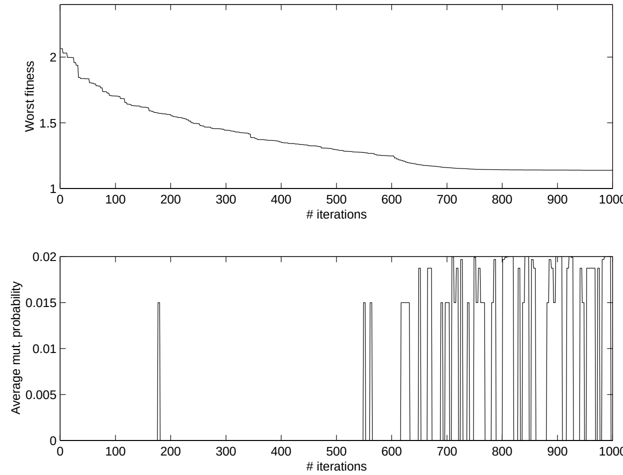

Figure 6. Ideal jet actuators, top: worst fitness in the population as a function of the optimization process iterations; bottom: mutation probability averaged over the population.

served for the velocities assigned to segments 3-4 and 13-14, also for this kind of actuators.

The other parameters are not so much clustered as in the tangential actuation case. This means that the segments containing the separation point are the most important ones in this case; however the solution yielded by the GA indicates that these segments (3-4 and 13-14) must always suck, so as to delay separation by allowing the flow to “slide” more on the cylinder surface. This confirms that the relevant feature for drag reduction is that the cylindrical segments containing the separation point have to perform either antisymmetric or symmetric actions, depending on the action considered.

Furthermore, the larger spreading of the population around the optimum that can be observed in this case suggests that the optimal actuation strength has not a critical value in the case of jet actuation, i.e. the tolerance on the actuation strength can be larger for the jet actuators. This fact can play a crucial role in the choice of which of these devices could be easier to be implemented in real world applications.

The time average of the vorticity contours near the cylinder, in fig. 8, show that the modification in the flow behavior due to this kind of actuation is very similar to the tangential actuation case.

5. Conclusions

A clustering Genetic Algorithm was used to study the drag reduction yielded by imposing a steady angular ve-

0-7695-0762-X/00 $10.00 © 2000 IEEE

locity profile to the boundary of a circular cylinder. The clustering feature of the algorithm allowed to examine the parameter correlations and to arrive at optimal velocity configurations, yielding a drag reduction of about 50%.

The genetic algorithm provides a systematic way to identify the significant parameters of the problem pertaining to critical points of the flow such as the separation points. An antisymmetric motion of segments near the separation points, directed in such a way so as to delay separation, has been found to be the most important feature of this active control system in the case of belt actuators, while a steady suction in correspondence of the same segments has been found to have the same effect. The first conclusion that can be drawn is that the GA confirmed quantitatively what common sense would suggest, i.e. in order to reduce the drag the flow should stay attached to the body surface as long as possible.

Another less trivial conclusion can be drawn by comparing the classes of solutions found for the two different kinds of actuation. From this comparison it emerges clearly that jet actuators yield a cost function with a shallower minimum basin, meaning that the tolerances for the jet actuation strengths can be larger than the tolerances needed for the belt actuators. This means that from this viewpoint jet actuators should be easier to implement.

The results of the algorithm demonstrate the capabilities of the proposed GA to efficiently solve drag minimization problems. The study presented in this paper can be also viewed as an evolutionary optimization method proceeding in an automatic, hierarchical fashion, by identifying the key parameters of the flow through the analysis of the minimum basin and further optimizing the parameters that appear more significant for the cost function. Physical insight and also useful hints for practical implementation can be obtained by observing the optimization route and the clustering of the actuator parameters.

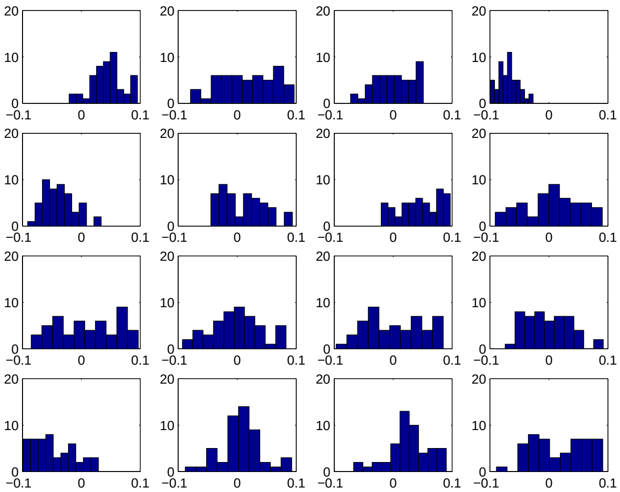

Figure 7. Population clustering, ideal jet actuators.

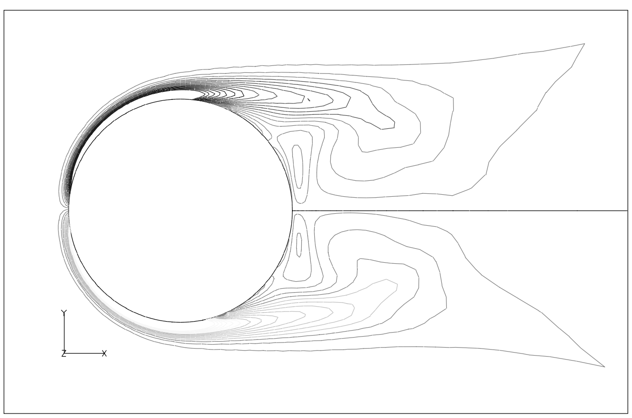

Figure 8. Ideal jet actuators: time averaged vorticity contours near the cylinder, control switched on.

References

[1] C. Apelt and G. West. The effects of wake splitter plates on bluff body flow in the range $10^4 < r < 5 \times 10^4$: Part 2. *J. Fluid Mech.*, 71:145, 1975.

[2] C. Apelt, G. West, and A. Szewczyk. The effects of wake splitter plates on bluff body flow in the range $10^4 < r < 5 \times 10^4$. *J. Fluid Mech.*, 61:187, 1973.

[3] D. Bechert, W. Hage, and M. Brusek. Drag reduction with the slip wall. *AIAA Journal*, 34(5), 1996.

[4] Y. Chen, Y. Ou, and A. Pealstein. Development of the wake behind a circular cylinder impulsively started into rotatory and rectilinear motion: Intermediate rotation rates. *J. Fluid Mech.*, 253:449, 1993.

[5] B. Choi and H. Choi. Drag reduction with a sliding wall in a flow over a circular cylinder. *AIAA Journal*, 38, 1999.

[6] J. Cimbala and S. Garg. Flow in the wake of a freely rotatable cylinder with splitter plate. *AIAA Journal*, 291:1001, 1991.

[7] D. Goldberg. *Genetic Algorithms in Search, Optimization, and Machine Learning*. Addison-Wesley, 1989.

[8] J. Holland. *Adaptation in Natural and Artificial Systems*. MIT Press, 1975.

[9] K. Kwon and H. Choi. Control of laminar vortex shedding behind a circular cylinder using splitter plates. *Phys. Fluids*, 8(2), 1996.

[10] C. Lee, J. Kim, and H. Choi. Suboptimal control of turbulent channel flow for drag reduction. *J. Fluid Mech.*, 358:245–258, 1998.

[11] M. Milano and F. Barone. An identification procedure performing automatic sensitivity analysis based on evolutionary programming. *IEEE Transactions on Systems, Man and Cybernetics*, 1999. Submitted, available at http://www.ifd.mavt.ethz.ch/members/Milano/.

[12] R. Mittal. Large-eddy simulation of flow past a circular cylinder. In *Annual Research Briefs*, page 107. Center for Turbulence Research, Stanford, 1995.

[13] V. Modi. Moving surface boundary layer control: a review. *Journal of Fluids and Structures*, 11, 1997.

[14] W. Price. A controlled random search procedure for global optimization. *The Computer Journal*, 20(4), 1976.

[15] I. Rechenberg. *Evolutionsstrategie*. Frommann-Holzboog, Berlin, 1994.

[16] A. Roshko. On the wake and drag of bluff bodies. *J. Aerosp. Sci.*, 22:124, 1955.

[17] M. Shumm, E. Berger, and P. Monkewitz. Self-excited oscillations in the wake of two dimensional bluff bodies and their control. *J. Fluid Mech.*, 271:17, 1994.

[18] P. Strykowsky and K. Sreenivasan. On the formation and suppression of vortex shedding at low reynolds numbers. *J. Fluid Mech.*, 218:71, 1990.

[19] P. Tokumaru and P. Dimotakis. Rotary oscillation control of a cylinder wake. *J. Fluid Mech.*, 224:77, 1991.

[20] M. Unal and D. Rockwell. On vortex formation from a cylinder. part 2. Control by splitter plate interference. *J. Fluid Mech.*, 190:513, 1987.